Postbuckling Behavior of Pressure- or Core-Stabilized Cylinders under Axial Compression

B. O. Almroth* and D. O. Brush†
Lockheed Missiles & Space Company, Palo Alto, Calif.

The postbuckling behavior of a circular cylindrical shell subjected to axial compression is considered in the presence of the stabilizing effects of internal pressure and of a soft elastic core. The classical buckling load and the minimum postbuckling equilibrium load may be considered as upper and lower bounds, respectively, for the actual buckling load. As expected, the analysis shows that these two bounds approach one another with increasing internal pressure or increasing core stiffness. A comparison with available test results indicates that most of the data fall within these converging bounds.

Nomenclature

a	=	cylinder radius
a_{ij}	=	constants [see Eq. (4)]
E	=	Young's modulus of shell
E_c	=	Young's modulus of core
E'	=	$(E_c/E)(a/t)^{3/2}$
F	=	stress function
f_{ij}	=	spring constants [see Eq. (7)]
L	=	cylinder length
l_x, l_ϕ	=	half wavelengths in axial and circumferential directions, respectively
p	=	internal pressure
$\bar{p}$	=	intersurface pressure [see Eq. (6)]
p'	=	$(p/E)(a/t)^2$
p_{ij}	=	constants [see Eq. (6)]
t	=	shell thickness
u,w	=	nondimensional axial and normal displacement components of a point in the shell's middle surface; corresponding distances are au and aw, and w is positive inward
V_c	=	potential energy of core
V_s	=	potential energy of shell (including external forces)
V	=	$V_s + V_c$
x	=	nondimensional coordinate in axial direction; corresponding distance is ax
z	=	wavelength parameter [see Eq. (13)]
ν	=	Poisson's ratio of shell
ν_c	=	Poisson's ratio of core
σ_0	=	classical buckling stress for empty cylinder
σ_{cr}	=	critical stress
$\sigma_x, \sigma_\phi, \tau_{x\phi}$	=	nondimensional stresses at a point in the middle surface of the shell; actual stresses are $E\sigma_x$, $E\sigma_\phi$, and $E\tau_{x\phi}$
ϕ	=	angular coordinate

Introduction

THE severe scatter in test results for axially compressed cylinders indicates that the buckling load is governed by at least one variable of chance character. Consequently, theoretical studies to determine the buckling load ultimately must incorporate an evaluation of the role of chance factors. However, it is possible to determine upper and lower bounds on the buckling load which are not sensitive to chance variations. The purpose of this paper is to determine such bounds for pressurized cylinders and for cylinders filled with a soft elastic core and to show that these bounds converge with increasing internal pressure or core stiffness.

Received March 20, 1963; revision received July 26, 1963. This work was carried out under the Lockheed Independent Research Program.

* Staff Scientist, Research Laboratories.
† Staff Scientist, Research Laboratories. Member AIAA.

Finite displacement analyses of axially loaded cylinders, such as that by Kempner,[1] lead to the load displacement relation illustrated in Fig. 1. Experimental evidence seems to indicate that there is little scatter in the magnitude of the minimum load in the postbuckling range. The minimum postbuckling load is the lowest load under which a buckled form of the cylinder can be maintained and will thus be considered as a lower bound for the buckling load. The classical buckling load, of course, is an upper bound for the critical load, although the work by Stein[2] suggests that it may not be the lowest upper bound.

For the empty cylinder the range between the lower and the upper bounds in general is quite wide, and present theoretical results are not directly useful. For pressurized cylinders and for cylinders filled with a soft elastic core, however, it will be shown that the difference between the classical buckling load and the minimum postbuckling load diminishes with increasing pressure or core stiffness. The load range within which buckling can occur thus becomes quite narrow for cylinders with a sufficient internal pressure or an elastic core of sufficient stiffness. Consequently, in some cases it may be possible to arrive at practically useful results through a postbuckling analysis of geometrically perfect cylinders, and thus avoid use of a statistical study of chance factors.

The classical buckling analysis of pressurized cylinders under axial compression leads to a critical load that is independent of the internal pressure. On the other hand, the minimum postbuckling load increases with increasing pressure, as has been shown in previous finite displacement analyses such as that of Ref. 3. Unfortunately, the numerical results of these analyses are unsatisfactory because the displacement function employed in the Rayleigh-Ritz analysis included too few degrees of freedom. With zero internal pressure, the analysis of Ref. 3 yields a minimum postbuckling load that is approximately three times higher than the corresponding experimental value.

An infinitesimal buckling analysis including the effect of a soft elastic core is available in Ref. 4 for cylinders under axial compression. A finite displacement analysis also has been performed,[5] but again in this case the displacement function contains too few degrees of freedom, and, furthermore, the core is assumed to act as a Winkler foundation.

In Ref. 6 an analysis of a cylinder without internal pressure or elastic core is presented, in which the number of degrees of freedom is successively increased until no significant change is observed in the minimum postbuckling load. The load so computed is in close agreement with available experimental evidence for the minimum postbuckling load. The complete postbuckling load-displacement curve was presented in Ref. 6 for four different displacement functions, which were labeled cases A, B, C, and D, respectively. Case A reproduces the results of Ref. 1. The others represent

various degrees of refinement of that analysis. The minimum postbuckling load in case D, with 11 degrees of freedom, is equal to 11% of the classical buckling load. In case C, with only 8 degrees of freedom, it is equal to 13% of the classical value, and hence case C may be considered a satisfactory approximation for the present purpose. Here, the analysis of Ref. 6 will be extended to include the additional effects of internal pressure and of a soft elastic core.

Basic Equations for the Pressurized Shell

An equation for the potential energy of a pressurized cylindrical shell without a core can be obtained by addition of a term representing the influence of internal pressure to the expression given, e.g., in Refs. 1 or 6 for the potential energy of the empty cylinder. Hence, the potential energy for the pressurized cylinder can be written:

$$V_s = \frac{Eta^2}{2}\left[\int_0^{L/a}\int_0^{2\pi}[(\sigma_x+\sigma_\phi)^2 - 2(1-\nu)(\sigma_x\sigma_\phi - \tau_{x\phi}^2)]dxd\phi + \frac{1}{12(1-\nu^2)}\times\left(\frac{t}{a}\right)^2\int_0^{L/a}\int_0^{2\pi}\left\{\left(\frac{\partial^2 w}{\partial x^2}+\frac{\partial^2 w}{\partial\phi^2}\right)^2 - 2(1-\nu)\left[\frac{\partial^2 w}{\partial x^2}\frac{\partial^2 w}{\partial\phi^2} - \left(\frac{\partial^2 w}{\partial x\partial\phi}\right)^2\right]\right\}dxd\phi - 2\int_0^{2\pi}\sigma_{x_{x=L/a}}d\phi\int_0^{L/a}\frac{\partial u}{\partial x}dx - 2\frac{p}{E}\cdot\frac{a}{t}\int_0^{L/a}\int_0^{2\pi}w dxd\phi\right] \quad (1)$$

The stresses here as well as the shell coordinates and the displacement components are nondimensional.

A stress function F is introduced such that

$$\sigma_x = \frac{\partial^2 F}{\partial\phi^2} \qquad \sigma_\phi = \frac{\partial^2 F}{\partial x^2} \qquad \tau_{x\phi} = -\frac{\partial^2 F}{\partial x\partial\phi} \quad (2)$$

The function can be expressed in terms of the normal displacement w by use of the compatibility equation:

$$\nabla^4 F = \left(\frac{\partial^2 w}{\partial x\partial\phi}\right)^2 - \frac{\partial^2 w}{\partial x^2}\frac{\partial^2 w}{\partial\phi^2} - \frac{\partial^2 w}{\partial x^2} \quad (3)$$

where

$$\nabla^4 = \left(\frac{\partial^2}{\partial x^2}+\frac{\partial^2}{\partial\phi^2}\right)^2$$

Assume that the normal displacement in the buckled configuration can be approximated by the expression

$$w = a_{00} + a_{20}\cos\frac{2a\pi x}{l_x} + a_{11}\cos\frac{a\pi x}{l_x}\cos\frac{a\pi\phi}{l_\phi} + a_{02}\cos\frac{2a\pi\phi}{l_\phi} + a_{40}\cos\frac{4a\pi x}{l_x} + a_{22}\cos\frac{2a\pi x}{l_x}\cos\frac{2a\pi\phi}{l_\phi} + a_{33}\cos\frac{3a\pi x}{l_x}\cos\frac{3a\pi\phi}{l_\phi} \quad (4)$$

Here l_x and l_ϕ are axial and circumferential half-wavelengths. The coefficient a_{00} can be determined from the condition that the tangential displacement must be a periodic function in ϕ. The remaining coefficients together with l_x and l_ϕ represent the generalized coordinates of the shell and will be determined through minimization of the total potential energy.

The forementioned displacement function, Eq. (4), differs slightly from the corresponding function in case C of Ref. 6. One term, which was included in case D, has been added and another has been dropped. Computations for the empty shell with use of Eq. (4) gives a minimum postbuckling load that is only 4% higher than that of case D. Consequently, Eq. (4) here gives an improvement in accuracy over case C, although the number of degrees of freedom is the same.

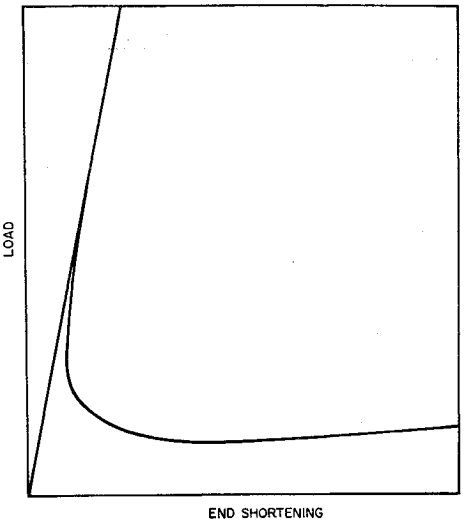

Fig. 1 Load displacement curve.

The forementioned equations together with the condition of stationary potential energy define equilibrium configurations in terms of nonlinear algebraic equations. These equations are solved by use of the Newton-Raphson iterative method.

Influence of an Elastic Core

The influence of a soft elastic core is accounted for through addition of the elastic energy of the core to the total potential energy of the system, Eq. (1). The authors now take advantage of the results in the analysis by Seide.[4] In that analysis, shearing stresses between core and shell are assumed to be negligible, so that restraint is offered only against normal displacements. A closed-form solution for the elastic support offered by the core is given in Ref. 4 only for the case of a core without a center hole, but it is indicated that a center hole has little effect if the hole radius is less than about half the cylinder radius.

Given a distribution of normal displacements on the surface of the core of the form

$$w = \Sigma_i\Sigma_j a_{ij}\cos(i\pi ax/l_x)\cos(i\pi a\phi/l_\phi) \quad (5)$$

one can find the corresponding surface pressure $\bar{p}$ through the equation

$$\bar{p} = \Sigma_i\Sigma_j p_{ij}\cos(i\pi ax/l_x)\cos(j\pi a\phi/l_\phi) \quad (6)$$

where

$$p_{ij} = [E_c/(1-\nu_c)]f_{ij}a_{ij} \quad (7)$$

The spring constants f_{ij}, as functions of the wavelengths, are given in Appendix A of Ref. 4. For the case $\nu_c = 0.5$, it was found numerically that if the wavelength in either direction is small compared to the circumference of the cylinder, the spring constants can be closely approximated by

$$f_{ij} = [(i\pi a/l_x)^2 + (j\pi a/l_\phi)^2]^{1/2} \quad (8)$$

As the numerical analysis is restricted here to core materials with $\nu_c = 0.5$, and the expected wavelengths are small compared with the circumference, this simplification is adopted for reasons of economy in the numerical analysis. An exception, of course, is for the case $i = j = 0$, for which Ref. 4 gives the solution:

$$f_{00} = (1+\nu_c)/(1-\nu_c) \quad (9)$$

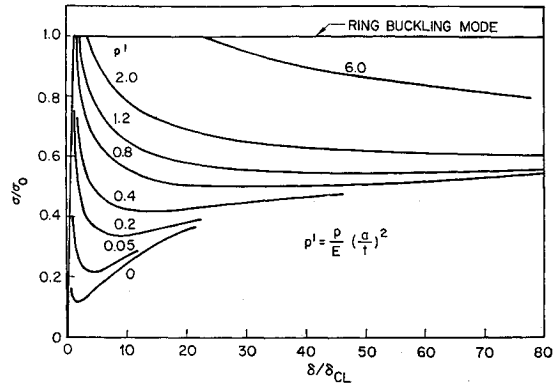

Fig. 2 Load displacement curves for pressurized cylinders.

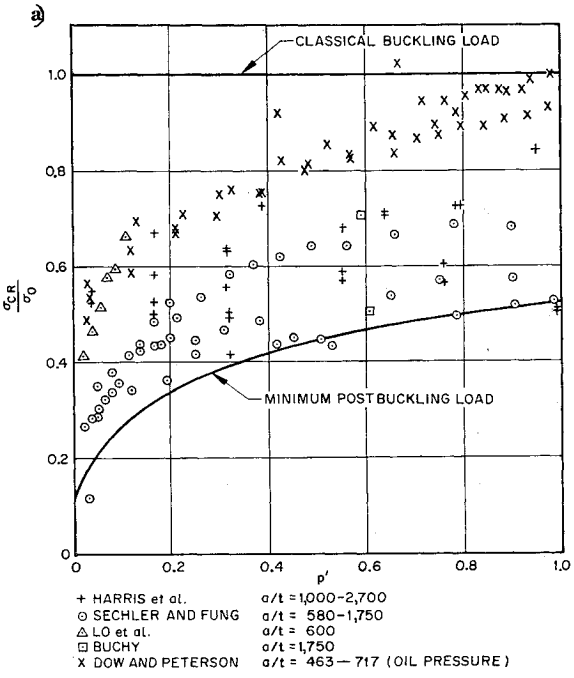

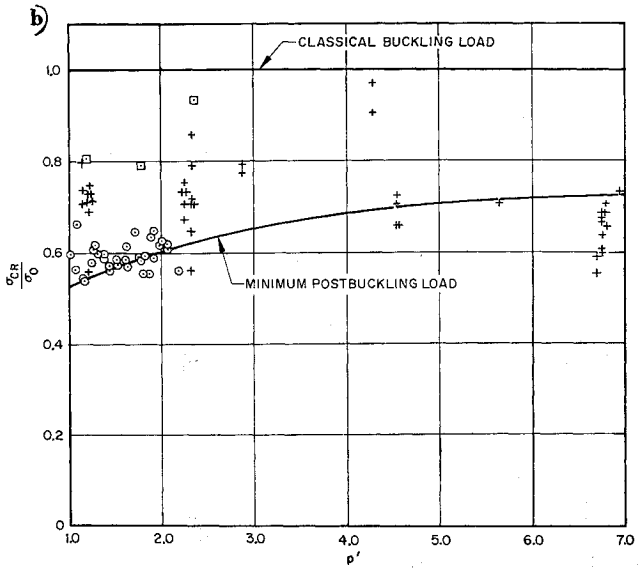

Fig. 3 a) Buckling of pressurized cylinders under axial compression ($0 < p' \leq 1.0$); b) buckling of pressurized cylinders under axial compression ($1.0 < p' \leq 7.0$).

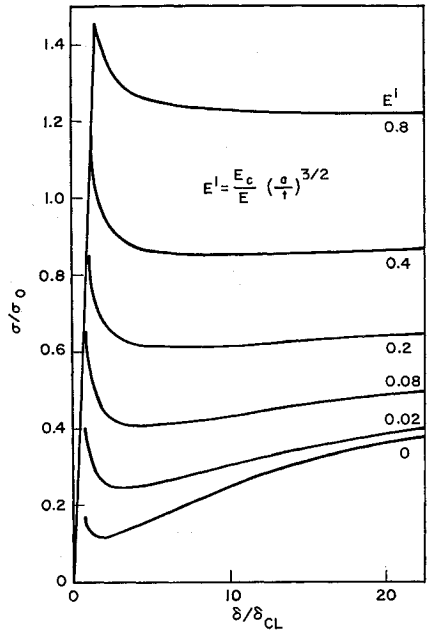

Fig. 4 Load displacement curves for core-filled cylinders.

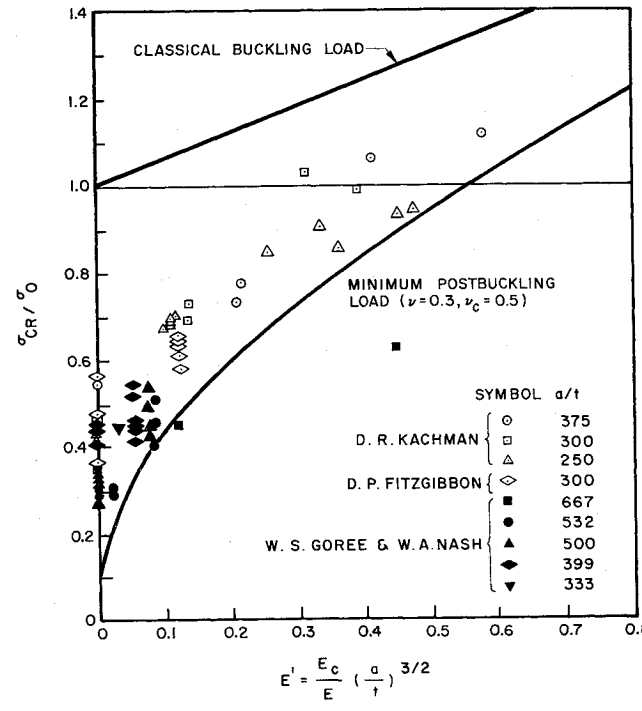

Fig. 5 Buckling of core-filled cylinders under axial compression.

As the strain energy of the core equals the work done by the forces on its surface, one has

$$V_c = \frac{1}{2}a^3 \int_0^{2\pi}\int_0^{L/a} w\,\bar{p}\,dx\,d\phi \tag{10}$$

where $\bar{p}$ represents the interface pressure. Thus, the core energy can be written

$$V_c = \frac{1}{2}a^3 \frac{E_c}{1-\nu_c}\int_0^{2\pi}\int_0^{L/a} \sum_i\sum_j\sum_n\sum_m f_{ij}\,a_{ij}\,a_{nm} \times \cos\left(\frac{i\pi ax}{l_x}\right)\cos\left(\frac{n\pi ax}{l_x}\right)\cos\left(\frac{j\pi a\phi}{l_\phi}\right)\cos\left(\frac{m\pi a\phi}{l_\phi}\right)dx\,d\phi \tag{11}$$

where the a_{ij}'s represent the coefficients in Eq. (4) and the f_{ij}'s are obtained from Eqs. (8) and (9).

The total potential energy of the system is given by the equation

$$V = V_s + V_c \tag{12}$$

The postbuckling equilibrium configurations are determined in the same manner as for the pressurized cylinder.

An equation for the classical buckling load can be obtained from these equations by deletion of nonlinear terms and minimization of V. This load supplies an upper bound for the critical load. Through minimization of σ with respect to the wave length parameter z, the classical buckling load is obtained from the equation:

$$8\sigma_{cr}z^2 = 2 + \frac{8}{3(1-\nu^2)}z^4 + \frac{8}{3}\frac{E_c}{E}\left(\frac{a}{t}\right)^{3/2}z \tag{13}$$

This result for the classical buckling load agrees with the corresponding result in Ref. 4.

Numerical Results

Load displacement curves were computed for the pressurized cylinder for various values of the internal pressure parameter $\bar{p}$. These curves are shown in Fig. 2. Although the classical buckling load is independent of $\bar{p}$ (ring buckling mode), it is seen that the minimum postbuckling load increases with this parameter. Similar results were obtained in Ref. 3, although in that analysis the minimum postbuckling load was overestimated grossly, because of the use of an inaccurate displacement function. The minimum postbuckling load is plotted vs $p' = (p/E)(a/t)^2$ in Fig. 3, together with test results. The test points shown in the figure include all results known to the authors for metal cylinders.[7-11] It may be seen that most of the points fall between the theoretical upper and lower bounds. However, at very high values of the internal pressure the test points have a tendency to fall below the minimum postbuckling load. One possible explanation is that for cases with very high internal pressure the minimum postbuckling load corresponds to such deep buckles that the present analysis is of questionable accuracy. However, it is also likely that many of the very low test points have been affected by plastic deformations due to excessive hoop stress. The tests by Dow and Peterson[11] show buckling loads that are considerably above the average from other experiments. This is at least partly due to the fact that their test cylinders were pressurized by oil, so that buckling was accompanied by a rise in internal pressure.

For cylinders with an elastic core, the fourth-order terms were retained in the expression for the potential energy of the core [Eq. (11)]. In this case the minimum postbuckling load, unlike the classical buckling load, is not a function of the parameter $E' = (E_c/E)(a/t)^{3/2}$ alone. However, the numerical analysis resulted in an insignificant difference between the postbuckling curves for cylinders with identical values of E' but with a/t varying within a wide range. Hence these fourth-order terms could have been excluded so that, for practical purposes, the results would depend only on E'. Accordingly, Fig. 4 shows load displacement curves for different values of the parameter E' alone. The classical buckling load and the minimum postbuckling load are shown as functions of E' in Fig. 5, together with test results taken from the compilation in Ref. 4. It is seen that the upper and lower bounds for the buckling load approach one another with increasing values of E', and that almost all of the test points fall between these bounds.

References

[1] Kempner, J., "Postbuckling behavior of axially compressed circular cylindrical shells," J. Aeronaut. Sci. **17**, 329–342 (1954).

[2] Stein, M., "The effect on the buckling of perfect cylinders of prebuckling deformations and stresses induced by edge support," NASA TN D-1510, pp. 217–227 (December 1962).

[3] Thielemann, W., "New developments in the non-linear theories of buckling of thin cylindrical shells," *Proceedings of the Durand Centennial Conference*, edited by N. J. Hoff and W. G. Vincenti (Pergamon Press, New York, 1960), pp. 76–119.

[4] Seide, P., "The stability under axial compression and lateral pressure of circular cylindrical shells with a soft elastic core," J. Aerospace Sci. **29**, 851–862 (1962).

[5] Lu, S. Y. and Nash, W. A., "Buckling of thin cylindrical shells stiffened by a soft elastic core," *Proceedings of the Colloquium on Simplified Calculation Methods*, edited by A. Paduart and R. Dutron (North-Holland Publishing Co., Amsterdam, 1961), pp. 475–481.

[6] Almroth, B. O., "Postbuckling behavior of axially compressed circular cylinders," AIAA J. **1**, 630–633 (1963).

[7] Harris, L. A., Suer, H. S., Skene, W. T., and Benjamin, R. J., "The stability of thin-walled unstiffened circular cylinders under axial compression including the effects of internal pressure," J. Aeronaut. Sci. **24**, 587–596 (1957).

[8] Fung, Y. C. and Sechler, E. E., "Buckling of thin-walled circular cylinders under axial compression and internal pressure," J. Aeronaut. Sci. **24**, 351–356 (1957).

[9] Lo, H., Crate, H., and Schwartz, E. B., "Buckling of thin-walled cylinder under axial compression and internal pressure," NACA Rept. 1027 (1951).

[10] Buchy, L. G., "Structural test of 70 inch diameter stainless steel integral propellant tank (stiffened)," North American Aviation Rept. AL-1154 (November 1950).

[11] Dow, M. B. and Peterson, J. P., "Bending and compression tests of pressurized ring-stiffened cylinders," NASA TN D-360 (April 1960).